

ELECTROVISCOUS FLOW THROUGH A MICROFLUIDIC T-JUNCTION

Joseph D. BERRY¹, Malcolm R. Davidson¹ and Dalton J. E. Harvie^{1*}

¹ Department of Chemical & Biomolecular Engineering, University of Melbourne, Parkville 3010, AUSTRALIA

*Corresponding author, E-mail address: daltonh@unimelb.edu.au

ABSTRACT

The steady-state electroviscous (pressure-driven) flow of an aqueous solution of potassium chloride through a microfluidic borosilicate glass T-junction is modelled using a finite volume approach. Electric-field propagation through the glass section of the T-junction is included in the analysis. Channel half-widths of 20-70 nm and salt concentrations of 0.01-1 M are considered. The hydrodynamic (pressure) and electrokinetic (electric potential) resistances of the T-junction are quantified in terms of equivalent lengths, and are shown to be a function of the dimensionless inverse Debye length K for intermediate values of K . For values of $K < 1$, both equivalent lengths of the junction are independent of K . For $K > 10$, the hydrodynamic equivalent length of the junction approaches the non-electrokinetic result. In contrast, the electrokinetic equivalent length of the junction increases with increasing K . For values of $K > 1$ and $W > 50$ nm, both equivalent lengths become independent of the channel half-width W .

NOMENCLATURE

A	Measured quantity (either potential or pressure)
dA/ds_{FD}	Fully-developed potential/pressure gradient
D	ion diffusivity
e	elementary charge
FD	fully-developed flow
K	dimensionless inverse Debye length
k	Boltzmann constant
L_{in}	length of inlet channel
L_{out}	length of outlet channel
$L_{eq,P}$	equivalent length based on pressure drop
$L_{eq,U}$	equivalent length based on potential drop
n_+	positive ion concentration
n_-	negative ion concentration
\mathbf{n}_{wall}	surface normal to wall, pointing into solid region
p	pressure
s	coordinate pointing in flow direction (parallel to wall)
T	temperature
U_f	fluid potential
U_w	solid potential
\mathbf{v}	velocity
W	channel half-width
\mathbf{x}	position
z	ion valence
ϵ_0	permittivity of free space
ϵ_f	fluid permittivity
ϵ_w	solid permittivity
μ	dynamic viscosity

ρ	density
ρ_E	charge density
σ	wall surface charge
Ω_f	fluid domain
Ω_w	solid domain

INTRODUCTION

Microfluidic lab-on-a-chip devices can be utilised to perform many applications, including the analysis and processing of biological fluids (Cheng et al., 2001.; Hatch et al., 2001; Squires et al., 2005). Many microfluidic devices utilise pumps to drive flow through networks of channels. Microfluidic pressure-driven flow can be subject to significant electrokinetic effects; depending on the channel dimensions, the conductivity of the fluids present and the materials used to manufacture the device. An effect known as electroviscosity describes the increased flow resistance due to the presence of mobile charge carriers within a fluid flowing through a microfluidic device with charged walls (Hunter, 1981).

In order to optimise the design of microfluidic devices, quantitative understanding of the pressure and potential changes occurring across network elements due to electroviscosity is required. Our group has characterised these changes in microfluidic contractions and microfluidic bends (Davidson and Harvie, 2007; Berry et al. 2011a, 2011b, 2012). This study investigates the effect of electroviscosity on low Reynolds number flow through a microfluidic 'T-junction'. A finite volume numerical method is used to simulate the flow through the T-junction. The effects of the channel dimensions and the salt concentration on the performance of the T-junction are quantified using equivalent lengths and compared to results for the conventional non-electrokinetic case.

MODEL FORMULATION

The steady-state, two-dimensional pressure-driven flow of a binary electrolytic fluid through a microfluidic T-junction is investigated (Fig. 1). The liquid is assumed to be an aqueous solution of potassium chloride with constant density, viscosity and permittivity; and anions and cations of equal and opposite valence and equal diffusivity. A constant surface charge density is assumed to be present on the channel walls. In practice the surface charge density can vary as a consequence of local conditions in the fluid (Schoch and Renaud, 2005). However, Stein et al. (2005) show that the constant surface charge assumption can give accurate predictions for flow through a microfluidic channel.

The physical properties used in the simulation are representative of typical microfluidic flows past borosilicate glass (Table 1). The electric-field propagation through the glass section of the T-junction is included, because it has been shown to have a significant effect on the flow dynamics of these systems (Berry et al., 2011b).

Property	Value
Temperature	298K
Viscosity ^a	8.91×10^{-4} Pa.s
Density ^a	1000 kg.m^{-3}
Fluid permittivity ^a	80.1
Solid permittivity ^a	4.6
Channel half-width	20-70 nm
Concentration	0.01-1 M
Ion diffusivity ^a	$2 \times 10^{-9} \text{ m}^2.\text{s}^{-1}$
Wall charge	-10 mC. m^{-2}
Flow velocity ^b	5 mm.s^{-1}

Table 1: Physical properties used in the model. (Based on flow of an aqueous solution of potassium chloride past borosilicate glass.) Notes: ^aEllis (1986), ^bJännig and Nguyen (2011)

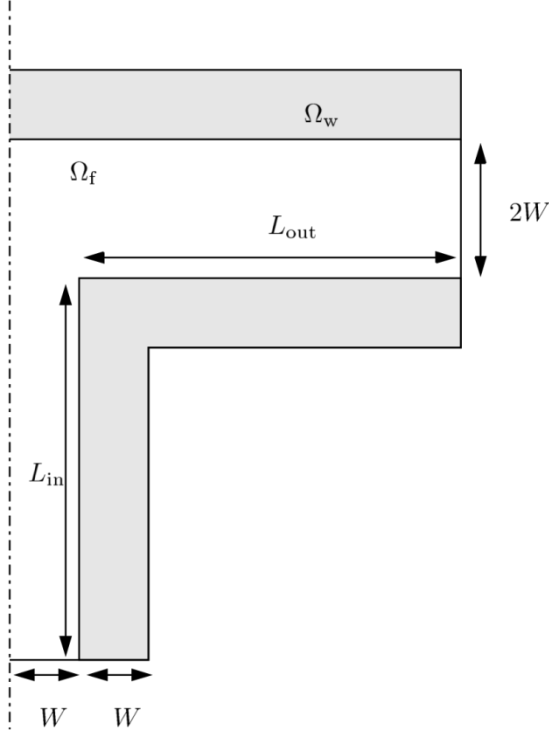


Figure 1: Schematic of T-junction geometry. The dashed-dotted line denotes the line of symmetry used in the simulations.

Governing Equations

The smallest channel half-width examined in this study is 20 nm. As a consequence, the ion transport and the fluid flow can be modelled using continuum dynamics (Daiguji, 2010). The continuum equations governing the steady flow in the fluid region Ω_f are

$$\nabla \cdot \mathbf{v} = 0, \quad (1)$$

$$\nabla \cdot (\rho \mathbf{v}) = -\nabla p + \nabla \cdot \mu [\nabla \mathbf{v} + (\nabla \mathbf{v})^T] - \rho_E \nabla U_f, \quad (2)$$

$$\nabla \cdot (n_{\pm} \mathbf{v}) = \nabla \cdot \left[D_{\pm} \nabla n_{\pm} + \frac{z_{\pm} e D_{\pm} n_{\pm}}{kT} \nabla U_f \right], \quad (3)$$

$$\nabla \cdot \epsilon_f \nabla U_f = -\frac{\rho_E}{\epsilon_0} = -\sum_{k=+,-} \frac{e z_k n_k}{\epsilon_0}, \quad (4)$$

where (1) is the continuity equation; (2) is the momentum equation; (3) is the ion transport equation for the anions and cations present in the fluid, and (4) is the Poisson equation for the electric potential. In the solid region, the electric potential satisfies

$$\nabla^2 U_w = 0. \quad (5)$$

Boundary Conditions

Across the channel wall the electric field normal to the wall undergoes a jump, given by

$$\epsilon_f \epsilon_0 \nabla U_f \cdot \mathbf{n}_{\text{wall}} - \epsilon_w \epsilon_0 \nabla U_w \cdot \mathbf{n}_{\text{wall}} = \sigma, \quad (6)$$

where \mathbf{n}_{wall} is the unit normal to the wall pointing into the solid region. Further, the electric potential is continuous across the wall:

$$U_f = U_w. \quad (7)$$

Along the external walls of the device, the gradient of electric potential is constrained in the direction normal to the wall by

$$\nabla U_w \cdot \mathbf{n}_{\text{wall}} = 0, \quad (8)$$

representing an interface with zero surface charge and no field propagation.

At the inlet and outlet of the channel, the velocity gradient normal to the flow, the concentration gradients normal to the flow, and the tangential velocity component are all set to zero. At the inlet, a flow-rate and the geometric mean ion number density $n_0 = \sqrt{n_+ n_-}$ are specified. The total current through the channel is set to zero, the necessary condition for electroviscous flow. The fluid/solid interface is set as a no-slip wall, with zero ion flux normal to the boundary.

Numerical Method

The governing equations (1)-(4) are solved in conjunction with the requisite boundary conditions on a composite structured/unstructured mesh generated with the program 'gmsh' (Geuzaine and Remacle, 2009). To ensure fully-developed flow at the inlet and outlet of the junction, $L_{\text{in}} = L_{\text{out}} = 15W$. For low values of W and n_0 , the development length of the flow is longer (Berry et al., 2001a), so in these instances it is necessary to set $L_{\text{in}} = 17.5W$. The fluid region Ω_f is meshed using rectangular elements, with 40 elements per channel half-width W . A typical mesh used in the simulation has $\sim 1.3 \times 10^5$ elements. The distribution of elements across the channel is non-uniform (Fig. 2), with fewer elements near

the centreline and more elements near the wall, in order to capture the high gradients of electric potential and salt concentrations in the electric double layer adjacent to the wall.

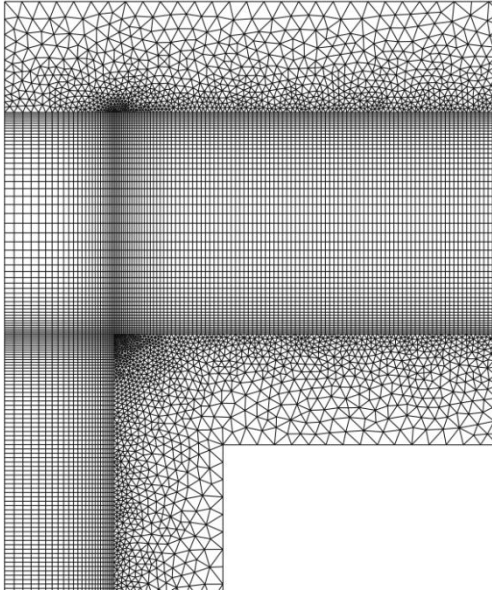


Figure 2: Coarse representation of the mesh used in the simulations. The structured section represents the fluid region Ω_f , and the unstructured section represents the solid region Ω_w .

The program ‘arb’ is used to cast the governing equations in finite volume form, and to find the corresponding steady-state solution using the Newton-Raphson method (Harvie, 2012). To validate the simulations, the pressure and potential gradients far upstream and downstream of the junction were compared to the one-dimensional solutions of the governing equations (Biscombe et al., 2012; Harvie et al., 2012). Very good agreement was obtained, with differences of less than 1% for the parameter space considered. Increasing the mesh resolution to 50 elements per half-width, or decreasing the resolution to 30 elements per half-width, changed the measured equivalent lengths by less than 1%.

RESULTS

Fig. 3a) shows a typical ion distribution for the flow through the T-junction. Electric double layers are present, with ions of opposite charge to the wall (counter-ions) present at very large concentrations near the wall. At this particular value of channel half-width W and salt concentration n_0 , the ions with the same charge as the wall (co-ions) are present at much lower concentrations than the counter-ions, even near the centre of the channel, due to the overlap of electric double layers. Because diffusion and conduction are the dominant means of ion transport, the size of the double layer is unaffected by the presence of the junction, with symmetry of the double layer present about the leading and trailing edge of the junction corner. (The Peclet number for the quantities modelled in this study ranges from 0.050 – 0.175).

Fig. 3b) compares a flow with ions present to a flow with no ions present (purely hydrodynamic flow). The streamlines show very little difference between the two flows, though there is a slightly higher flow velocity at the

centreline of the flow with ions present due to the electroviscous effect. From the pressure contours however it is clear that the characteristics of electroviscous flow are quite different from purely hydrodynamic flow, with significant variation of the pressure across the channel width.

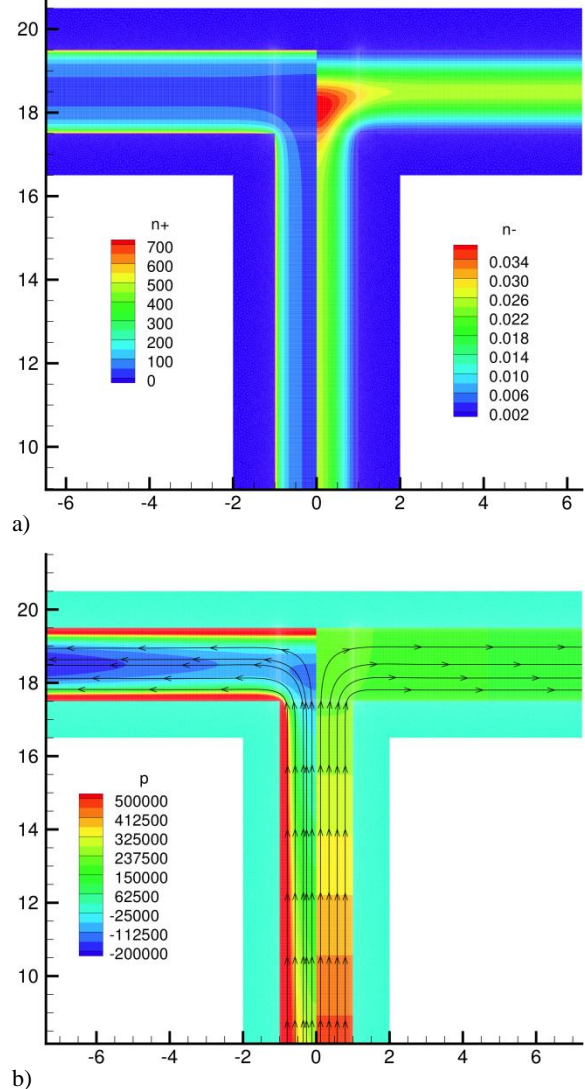


Figure 3: a) Distribution of counter-ions (left) and co-ions (right) in the T-junction for $n_0 = 0.1$ M. b) Contours of pressure and streamlines for $n_0 = 0.1$ M (left) and purely hydrodynamic flow (right). Note that the maximum pressure contour depicted is much lower than the pressure near the wall for the case where ions are present. For both T-junctions shown the channel half-width $W = 20$ nm, and the axes have been normalised with length-scale W . All physical properties are listed in Table 1.

The hydrodynamic and electrokinetic resistance of the T-junction to the flow can be quantified using equivalent lengths. These are defined as the length of uniform inlet channel (with half-width W) needed to match the pressure (potential) drop caused by the effect of the T-junction (Berry et al., 2011b). Formally, these equivalent lengths are defined as

$$L_{eq,A} = \frac{\Delta A - \sum_{k=in,out} L_k \frac{dA}{ds} \Big|_{FD,k}}{\frac{dA}{ds} \Big|_{FD,in}}, \quad (9)$$

where A is either the pressure or the potential. This definition is valid only if ΔA is measured over a length beginning and ending in fully-developed flow regions in the inlet and outlet respectively.

The equivalent lengths based on the pressure and potential drop of the T-junction are given in Fig. 4 for a range of channel half-widths and salt concentrations.

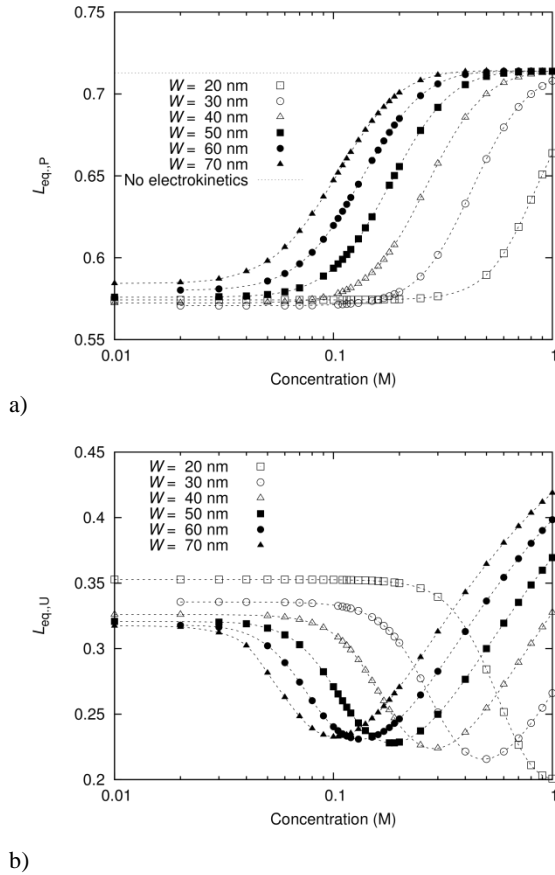


Figure 4: Equivalent length of the T-junction based on a) the pressure drop over the geometry, and b) the potential drop over the geometry, as a function of average salt concentration. The flow velocity is 5 mm/s, and the wall surface charge is -10 mC.m^{-2} . Each symbol represents a simulation result. The lines are spline fits to the data presented.

For low to intermediate concentrations, the equivalent lengths are constant, and dependent on the size of the channel half-width W . This effect diminishes with increasing W . As the concentration increases, the equivalent length based on the pressure, $L_{eq,P}$, increases monotonically towards the $L_{eq,P}$ value given by purely hydrodynamic flow.

The equivalent length based on the potential, $L_{eq,U}$, decreases with increasing concentration until a minimum resistance is reached, whereupon the equivalent length

then increases monotonically with concentration. The concentration at which the minimum resistance is incurred decreases with increasing channel half-width W .

To explain the dependence of the equivalent lengths on both the concentration and channel half-width, the results can be presented in terms of

$$K = \left[\frac{2z^2 e^2 n_0 W^2}{\epsilon \epsilon_r k T} \right]^{\frac{1}{2}}, \quad (10)$$

which is the dimensionless inverse Debye length. This parameter can also be interpreted as the square root of a dimensionless concentration. When K is small, the thickness of the electric double layer is greater than the channel dimension, and significant overlap occurs. At this limit, there is a nearly constant amount of charge (opposite and equal to the fixed surface charge) across the channel due to the exclusion of co-ions, and no region of electrically neutral fluid. When K is large, the double layer thickness is small in comparison with the channel dimension, and all the charge present in the flow is located in a thin region adjacent to the wall. As a result, the bulk flow is electrically neutral.

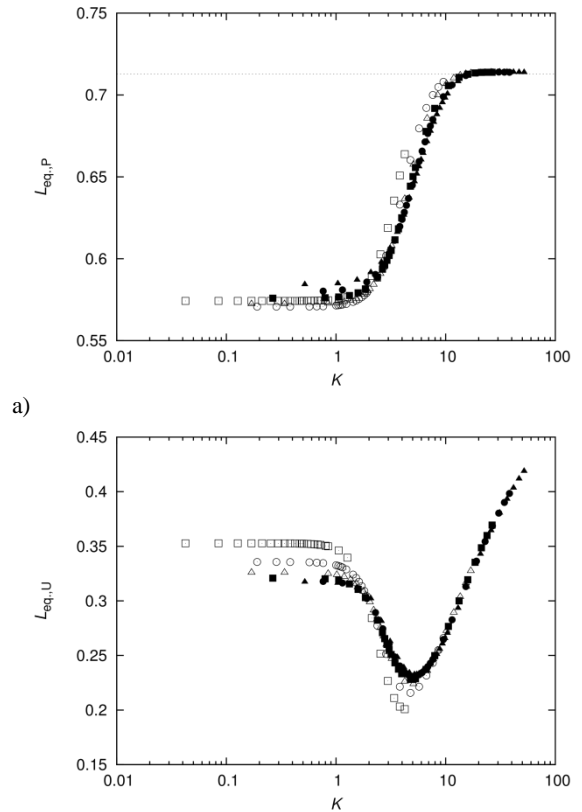


Figure 5: Equivalent length of the T-junction based on a) the pressure drop over the geometry, and b) the potential drop over the geometry, as a function of dimensionless inverse Debye length K . The symbols represent the same channel half-widths given in Fig. 4.

For values of $K < 1$ both equivalent lengths are dependent upon the channel half-width W ; but independent of K due

to the exclusion of co-ions in the channel, and the consequent fixed charge therein. As the double layer thickness becomes comparable to the channel dimension however, the resistance of the junction begins to vary with K . As K increases, so does $L_{eq,p}$. For values of $K > 10$ the fluid bulk is electrically neutral, and as a consequence the equivalent length based on the pressure is the same as the equivalent length calculated for purely hydrodynamic flow. Interestingly, for values of $K > 1$ and $W > 50\text{nm}$, the equivalent length based on the pressure is independent of W .

The equivalent length of the T-junction based on the potential displays similar behaviour for $K < 1$. For increasing values of K above 1, $L_{eq,U}$ decreases until a minimum resistance is reached at $K \sim 5$. As K increases further, the double layer decreases in thickness, and electrokinetic effects decrease. Consequently, the potential drop caused by the junction (numerator of Eq. 9), and the potential drop per unit length of uniform channel (denominator of Eq. 9) go to zero as $K \rightarrow \infty$. However, upon inspection of the data, the potential drop caused by the junction goes to zero more slowly than the potential drop per unit length of uniform channel, resulting in $L_{eq,U}$ increasing as the double layer becomes thinner. Again, for values of $K > 1$ and $W > 50\text{nm}$, the magnitude of $L_{eq,U}$ becomes independent of the channel half-width W .

CONCLUSION

The steady-state pressure-driven flow of an aqueous solution of potassium chloride through a T-junction has been studied for a range of channel dimensions and salt concentrations. The resistance of the junction to the flow has been quantified in terms of equivalent lengths based upon the pressure and potential drops over the junction. The equivalent lengths of the junction are a function of the dimensionless inverse Debye length K . For thick double layers, $K < 1$, the equivalent lengths based upon both the pressure and potential are constant. For values of $K > 1$, the pressure equivalent length increases monotonically, whereas the potential equivalent length decreases to a minimum at $K \sim 5$. For thin double layers, $K > 10$, the pressure equivalent length approaches the equivalent length for purely hydrodynamic flow, however the potential equivalent length continues to increase. For values of $K > 1$ and $W > 50\text{ nm}$, the equivalent lengths become independent of the channel half-width W within the range of W studied.

ACKNOWLEDGMENTS

This research was supported by the Australian Research Council Grants Scheme and by computational resources on the National Computational Infrastructure Facility through the National Computational Merit Allocation Scheme.

REFERENCES

BERRY, J.D., DAVIDSON, M.R. and HARVIE, D.J.E., (2011a), "Electrokinetic development length of electroviscous flow through a contraction", *ANZIAM J.*, 52, C837–C852.
 BERRY, J.D., DAVIDSON, M.R. and HARVIE, D.J.E., (2011b), "Effect of wall permittivity on electroviscous flow through a contraction", *Biomicrofluidics*, 5,

044102.

BERRY, J.D., FOONG, A.E., LADE, C., ROSS, E., FAISAL, E.E., BISCOMBE, C.J.C., DAVIDSON, M.R. and HARVIE, D.J.E., (2012) "Electroviscous flow through microfluidic bends", in *preparation for Colloid Surface A*
 BISCOMBE, C.J.C., HARVIE, D.J.E. and DAVIDSON, M.R., (2012), "Microfluidic circuit analysis II: Implications of ion conservation in series circuits", *J. Colloid Interface Sci*, 365, 16-27
 CHENG, S. B., SKINNER, C. D., TAYLOR J., ATTIYA, S., LEE, W. E., PICELLI, G. and HARRISON, D. J., (2001), "Development of a multichannel microfluidic analysis system employing affinity capillary electrophoresis for immunoassay", *Anal. Chem.*, 73(7), 1472–1479.
 DAIGUJI, H., (2010), "Ion transport in nanofluidic channels", *Chem. Soc. Rev.*, 39, 901-911
 DAVIDSON, M.R. and HARVIE, D.J.E., (2007) "Electroviscous effects in low Reynolds number liquid flow through a slit-like microfluidic contraction", *Chem. Eng. Sci.*, 62, 4229–4240.
 ELLIS, H. (Ed.), (1986), "Book of Data", 4th ed., Longman Group Limited, Harlow
 GEUZAIN, C. and REMACLE, J.-F., (2009), "Gmsh: A 3-d finite element mesh generator with built-in pre- and post-processing facilities", *Int. J. Numer. Meth. Eng.*, 79(11), 1309–1331.
 HARVIE, D.J.E., (2012), "An implicit finite volume method for arbitrary transport equations", *ANZIAM J.*, C1126-C1145.
 HARVIE, D.J.E., BISCOMBE, C.J.C. and DAVIDSON, M.R., (2012), "Microfluidic circuit analysis I: Ion current relationships for thin slits and pipes", *J. Colloid Interface Sci*, 365, 1-15
 HATCH, A., KAMHOLZ, A. E., HAWKINS, K. R., MUNSON, M. S., SCHILLING, E. A., WEIGL, B. H. and YAGER, P., (2001), "A rapid diffusion immunoassay in a t-sensor", *Nat. Biotechnol.*, 19(5), 461–465.
 HUNTER, R. J., (1981), "Zeta Potential in Colloid Science", Academic Press, London, 1981.
 JÄNNIG, O. and NGUYEN, N.-T., (2011), "A polymeric high-throughput pressure-driven micromixer using a nanoporous membrane", *Microfluid. Nanofluid.*, 10, 513–519
 SCHOCH, R. B. and RENAUD, P., (2005), "Ion transport through nanoslits dominated by the effective surface", *App. Phys. Lett.*, 86(25), 253111
 STEIN, D., KRUIHOF, M. and DEKKER, C., (2004), "Surface-charge-governed ion transport in nanofluidic channels", *Phys. Rev. Lett.*, 93(3), 1-4
 SQUIRES, T. M. and QUAKE, S.R., (2005), "Microfluidics: fluid physics at the nanoliter scale", *Rev. Mod. Phys.*, 77(3), 977–1026.